P-Rex2 regulates Purkinje cell dendrite morphology and motor coordination

Sarah Donald*, Trevor Humby[†‡], Ian Fyfe*, Anne Segonds-Pichon[§], Simon A. Walker[¶], Simon R. Andrews[§], W. John Coadwell[§], Piers Emson[‖], Lawrence S. Wilkinson[†‡], and Heidi C. E. Welch*[,**]

*Inositide Laboratory, [†]Laboratory for Cognitive and Behavioural Neuroscience, [§]Bioinformatics Group, [¶]Imaging Facility, and [‖]Laboratory for Molecular Neuroscience, The Babraham Institute, Babraham Research Campus, Cambridge CB22 3AT, United Kingdom

Communicated by Michael J. Berridge, The Babraham Institute, Cambridge, United Kingdom, January 2, 2008 (received for review October 9, 2007)

The small GTPase Rac controls cell morphology, gene expression, and reactive oxygen species formation. Manipulations of Rac activity levels in the cerebellum result in motor coordination defects, but activators of Rac in the cerebellum are unknown. P-Rex family guanine-nucleotide exchange factors activate Rac. We show here that, whereas P-Rex1 expression within the brain is widespread, P-Rex2 is specifically expressed in the Purkinje neurons of the cerebellum. We have generated P-Rex2$^{-/-}$ and P-Rex1$^{-/-}$/P-Rex2$^{-/-}$ mice, analyzed their Purkinje cell morphology, and assessed their motor functions in behavior tests. The main dendrite is thinned in Purkinje cells of P-Rex2$^{-/-}$ pups and dendrite structure appears disordered in Purkinje cells of adult P-Rex2$^{-/-}$ and P-Rex1$^{-/-}$/P-Rex2$^{-/-}$ mice. P-Rex2$^{-/-}$ mice show a mild motor coordination defect that progressively worsens with age and is more pronounced in females than in males. P-Rex1$^{-/-}$/P-Rex2$^{-/-}$ mice are ataxic, with reduced basic motor activity and abnormal posture and gait, as well as impaired motor coordination even at a young age. We conclude that P-Rex1 and P-Rex2 are important regulators of Purkinje cell morphology and cerebellar function.

G protein-coupled receptor | guanine-nucleotide exchange factor | phosphoinositide-3-kinase | small GTPase Rac | ataxia

The small GTPase Rac (isoforms 1, 2, and 3) controls the structure of the actomyosin cytoskeleton, gene expression, and reactive oxygen species (ROS) formation (1). In the nervous system, Rac is essential for all stages of neuronal development (neurite, axon, and dendrite formation, axon pathfinding, dendrite branching and dendritic spine formation, and survival), as shown by manipulations of Rac activity in the nervous system of animals, neuronal cell lines, and primary cultures (2).

Deletion of the ubiquitous Rac1 from the mouse, whether total or specifically in the brain, is embryonic lethal (3, 4), but transgenic overexpression of constitutively active Rac1 in the Purkinje neurons of the cerebellum results in severe ataxia, with animals unable to walk in a straight line and poor performance on the rotarod (5). Similarly, deletion of nervous system-specific Rac3 results in an increased ability for learning and coordination of skilled movements (6), deletion of the Rac-GAP α-Chimerin induces a hopping gait due to misguidance of corticospinal tract axons (7), and deletion of the brain-specific form of the Rac-effector Wave, which links Rac to the actin cytoskeleton, causes defects in motor coordination, learning, and memory (8).

Like all small GTPases, Rac is activated by guanine-nucleotide exchange factors (GEFs) (9). Several Rac-GEFs are known to control neuronal development: Tiam1/Stef regulates neurite and axon outgrowth and dendritic spine formation (2, 10); Vav2 and Vav3 control axon outgrowth from retina to thalamus (11); Trio governs neurite outgrowth, axon extension, and pathfinding (2); Kalirin regulates neurite and axon outgrowth and dendritic spine formation (2); Dock180 controls neurite outgrowth (12) and Dock7, axon formation (13); GEFT and βPIX regulate dendritic spine formation (14, 15); and Alsin regulates neuronal survival (16, 17). Which GEFs activate Rac in the cerebellum is unknown.

The P-Rex family of Rac-GEFs differs from others in their mode of regulation: they are synergistically activated by the $\beta\gamma$-subunits of heterotrimeric G proteins and by the phosphatidylinositol (3, 4, 5)-trisphosphate that is generated by phosphoinositide-3-kinase (PI3K), as coincidence detectors for the stimulation of G protein-coupled receptors (GPCRs) and PI3K (18). The P-Rex family comprises P-Rex1, P-Rex2, and P-Rex2b (18–20). Northern blots suggest that P-Rex1 is expressed in white blood cells and brain (18), P-Rex2 more widely but not in leukocytes (19), and P-Rex2b, a splice variant of P-Rex2, only in the heart (20). P-Rex1 regulates GPCR-dependent Rac2 activation, ROS production, and chemotaxis in neutrophils, and neutrophil recruitment to inflammatory sites (21, 22). In PC12 cells, P-Rex1 controls neurotrophin-stimulated cell migration (23). In HUVEC cells, P-Rex2b governs Rac1 activation and cell migration in response to sphingosine 1-phosphate (24). The functional importance of P-Rex2 is unknown. To study it, we have generated P-Rex2$^{-/-}$ and P-Rex1$^{-/-}$/P-Rex2$^{-/-}$ mice and analyzed the effects of P-Rex deficiency on Purkinje cell morphology and mouse behavior. We report that the P-Rex Rac-GEF family controls cerebellar morphology and function.

Results

P-Rex2-Deficient Mice Are Viable and Fertile and Appear Healthy. We have generated P-Rex2-deficient mice by using the gene-trapped embryonic stem cell line RRD186 from BayGenomics that has a pGT1Lxf-targeting vector insertion between exons 34 and 35 of mouse P-Rex2 (supporting information (SI) Figs. 7 and 8). P-Rex2$^{-/-}$ animals were obtained with the expected Mendelian frequency, viable, fertile, and apparently healthy. They had normal longevity, normal body weight at a young age, and normal appearance and weight of major organs (SI Fig. 8*C*), although P-Rex2$^{-/-}$ females developed significantly lower body weight than controls later in life (SI Fig. 8*D*).

P-Rex2 Protein Is Expressed in Brain and Lung. We raised sheep polyclonal antibodies against peptide 794–805 of mouse P-Rex2 and rabbit polyclonal antibodies against amino acids 717–799 of mouse P-Rex2 and affinity purified them (SI Fig. 9*A*). Western blots using the sheep antibodies revealed that, in adult wild-type (Wt) mice, P-Rex2 protein is abundant in brain and lung. Low-level expression was detectable in liver, thymus, and spleen (Fig. 1*A*).

Author contributions: S.D., T.H., S.R.A., W.J.C., P.E., L.S.W., and H.C.E.W. designed research; S.D., I.F., and H.C.E.W. performed research; P.E. and H.C.E.W. contributed new reagents/analytic tools; S.D., T.H., A.S.-P., S.A.W., S.R.A., W.J.C., and H.C.E.W. analyzed data; and S.D. and H.C.E.W. wrote the paper.

The authors declare no conflict of interest.

[‡]Present address: Behavioural Genetics Group, at School of Psychology and Department of Psychological Medicine, School of Medicine, Cardiff University, Cardiff CF10 3AT, United Kingdom.

**To whom correspondence should be addressed. E-mail: heidi.welch@bbsrc.ac.uk.

This article contains supporting information online at www.pnas.org/cgi/content/full/0712324105/DC1.

PHYSIOLOGY

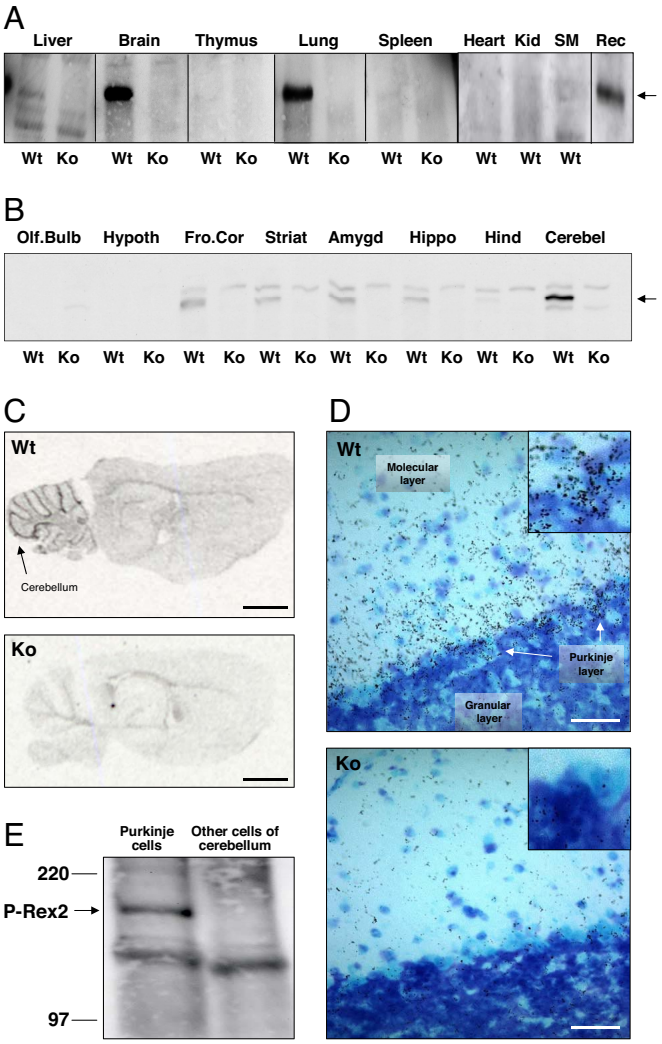

Fig. 1. P-Rex2 is expressed in the Purkinje neurons of the cerebellum. (*A*) Tissue distribution of P-Rex2 in adult Wt mice (and deletion in P-Rex2$^{-/-}$ mice, Ko), determined by Western blotting of total lysates with affinity-purified sheep P-Rex2 antibody. Equal amount of protein per lane. Rec = 100 ng of purified recombinant human EE-tagged P-Rex2 (19). (*B*) P-Rex2 Western blot of mouse brain section lysates from adult P-Rex2$^{+/+}$ (Wt) and P-Rex2$^{-/-}$ (Ko) mice by using affinity-purified rabbit P-Rex2 antibody; 500 μg of tissue per lane. (*C*) *In situ* hybridization of adult P-Rex2$^{+/+}$ (Wt) and P-Rex2$^{-/-}$ (Ko) mouse brain sections with a probe to base pairs 4765–4804 of mouse P-Rex2. Slides are representative of four. (Scale bar, 2 mm.) (*D*) Silver emulsion staining of P-Rex2$^{+/+}$ (Wt) and P-Rex2$^{-/-}$ (Ko) slides as in *C*, focused on the Purkinje cell body region at the boundary of granular layer (densely blue-stained granule cell bodies) and molecular layer (light blue, contains Purkinje cell dendrites). (Scale bars, 50 μm.) (*Insets*) Twofold magnification of the three-layer interface. Slides are representative of five sections. (*E*) P-Rex2 Western blot (rabbit antibody) on total lysates of EGFP-high Purkinje cells and EGFP-low other cerebellar cell types isolated by FACS sorting from cerebellar cell suspension from 4-week-old pups of EGFP-Pcp2 mice (25). Equal amounts of protein per lane. Blot is representative of two blots from separate experiments.

Essentially the same results were obtained with the rabbit antibodies (data not shown). Hence, the distribution of P-Rex2 protein is more restricted than expected from Northern blot analysis (19). P-Rex2 protein was deleted in the P-Rex2$^{-/-}$ mouse (Fig. 1*A*).

Within the Brain, P-Rex2 Is Expressed in the Purkinje Neurons of the Cerebellum. P-Rex2$^{-/-}$ mouse brains showed no obvious anatomical defects (data not shown). Western blotting of brain sections revealed that P-Rex2 expression is highly concentrated in the cerebellum, although low-level expression was detected in the frontal cortex, striatum, amygdala and hippocampus (Fig. 1*B*), but at least fivefold lower than in cerebellum, as judged by densitometric scanning and National Institutes of Health ImageJ analysis. Cerebellar P-Rex2 expression was detectable in pups from 5 days of age, increased until at least 17 days of age, and stayed high throughout life (SI Fig. 9*B*, and data not shown). Expression of P-Rex2 was abrogated in the P-Rex2$^{-/-}$ brain (Fig. 1*B*).

In situ hybridization showed that, like P-Rex2 protein, P-Rex2 mRNA was highly restricted to the cerebellum and deleted in P-Rex2$^{-/-}$ mice (Fig. 1*C*). Similar results were obtained with four different probes (data not shown). Silver-emulsion labeling of the *in situ* hybridization slides gave P-Rex2 signal in the Purkinje neuron layer and within the molecular layer that contains the dendrites of Purkinje cells (Fig. 1*D*), suggesting that P-Rex2 may be expressed in Purkinje neurons. To confirm this, we used transgenic mice expressing EGFP under a Purkinje cell-specific promoter, Pcp2 (25). We FACS-sorted their EGFP-positive Purkinje neurons from other cell types in a cerebellar suspension (25) and Western blotted both populations for P-Rex2 expression. Indeed, P-Rex2 protein was found specifically in Purkinje cells (Fig. 1*E*).

Purkinje Cell Dendrite Morphology Is Altered in P-Rex2$^{-/-}$ Mice. To look for potential morphological defects in Purkinje cells from P-Rex2$^{-/-}$ mice, we crossed P-Rex2$^{-/-}$ and Pcp2-EGFP mice to obtain mice with fluorescent green Purkinje cells and either P-Rex2$^{-/-}$ or P-Rex2$^{+/+}$, and analyzed cerebellar slices by confocal microscopy. The cerebellar morphology of EGFP-P-Rex2$^{-/-}$ mice and alignment of Purkinje cells between the granular and molecular layers appeared normal. Equally, axon and dendrite outgrowth in the developing Purkinje cells of EGFP/P-Rex2$^{-/-}$ pups (Fig. 2*A*), dendrite branching, and dendritic spine formation appeared largely as in EGFP/P-Rex2$^{+/+}$ littermate pups (Fig. 2*B* and SI Fig. 10 *A* and *B*).

To analyze the morphology of mature Purkinje cells, we prepared cerebellar slices from adult P-Rex2$^{-/-}$ and P-Rex2$^{+/+}$ animals, stained for the Purkinje cell marker Calbindin, and analyzed slices by confocal fluorescence microscopy. This revealed that Purkinje cell dendrite structure is abnormal in adult P-Rex2$^{-/-}$ mice (Fig. 2*C*): the main dendritic trunk appeared shriveled and unordered in P-Rex2$^{-/-}$ cells. Compared with Wt cells, the base of the main trunk was only clearly visible in half the P-Rex2$^{-/-}$ cells, whereas the width of the molecular layer was normal (Fig. 2 *C* and *D*). The defect persisted throughout adulthood and was similar in 3- and 20-month- old animals (Fig. 2*D*).

To investigate the likely underlying cause for this defect, we analyzed high-resolution confocal Purkinje cell image stacks from 18-day-old EGFP-P-Rex2$^{-/-}$ and EGFP-P-Rex2$^{+/+}$ mice by using Volocity software (Fig. 2 *E* and *F* and SI Fig. 10). This showed that the diameter of the P-Rex2$^{-/-}$ main Purkinje cell dendrite was reduced by ≈20% (Fig. 2*E*). In addition, the length of the main Purkinje cell dendrite (to a major branch point), although highly variable between cells, showed a tendency to be shorter in P-Rex2$^{-/-}$ mice (SI Fig. 10*B* and Fig. 2*F*). Hence, Purkinje cell dendrite structure is impaired in pups and adult P-Rex2$^{-/-}$ mice.

P-Rex2 Deficiency Causes a Motor Coordination Defect. The cerebellum regulates the learning and coordination of skilled movements (26, 27). Cerebellar defects, either through injury or degenerative genetic disorders, such as spinocerebellar ataxia, manifest themselves as disturbances of posture and voluntary movement (28). To reveal a potential role of P-Rex2 in motor coordination, we examined P-Rex2$^{-/-}$ mouse behavior by using an established battery of neurological tests for cerebellar dysfunction. We tested a cohort of 53 P-Rex2$^{-/-}$ and P-Rex2$^{+/+}$ mice (at least 12 males and 12 females per group) at 2, 6, 9, 12, and 15 months of age.

The classic test for mouse motor coordination is the rotarod test (SI Movie 1) (29). Although learning to run on the rotarod was

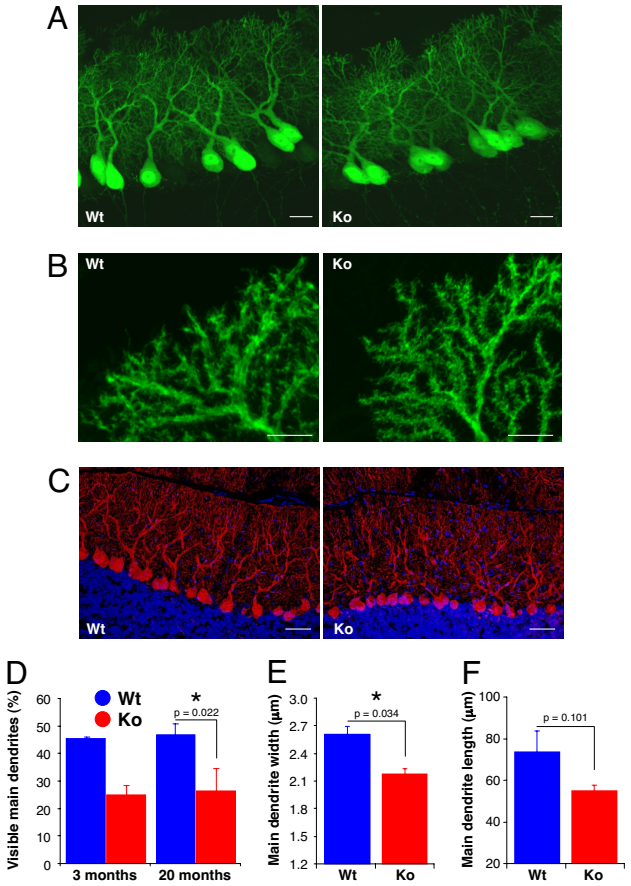

Fig. 2. P-Rex2$^{-/-}$ mice have a defect in Purkinje cell dendrite morphology. (*A* and *B*) Cerebellar slices from 10-day-old EGFP-P-Rex2$^{-/-}$ (Ko) and littermate control EGFP-P-Rex2$^{+/+}$ (Wt) mice were fixed and analyzed by confocal microscopy. (*A*) Purkinje cell alignment and axon and dendrite outgrowth in EGFP-P-Rex2$^{-/-}$ mice. (Scale bars, 20 μm.) (*B*) Purkinje cell dendritic branches in EGFP-P-Rex2$^{-/-}$ mice. Photos are representative of three sections from at least three mice per genotype. (Scale bars, 10 μm.) (*C*) Cerebellar slices from 3-month-old P-Rex2$^{-/-}$ (Ko) and P-Rex2$^{+/+}$ (Wt) mice were fixed, permeabilized, and stained for Calbindin (red) and with Hoechst (blue). Photos are representative of three slices (≈500 Purkinje cells each) per genotype. (Scale bars, 50 μm.) (*D*) Quantification of P-Rex2$^{-/-}$ (Ko, red) and P-Rex2$^{+/+}$ (Wt, blue) Purkinje cell dendrite structure. Cerebellar slices as in *C* from 3- and 20-month-old mice were scored by microscopy for the percentage of Purkinje cells with a clearly visible main dendritic trunk when focused on the cell body. Data are from at least two slices per animal, one animal per genotype for 3-month-old and three animals per genotype for 20-month-old mice. Values are mean ± range blind scores of two people. (*E* and *F*) Volocity analysis of high-resolution confocal image stacks of cerebellar slices from18-day-old EGFP-P-Rex2$^{-/-}$ (Ko) and littermate EGFP-P-Rex2$^{+/+}$ (Wt) mice, three animals per genotype from two litters of different origins. Data are mean ± SE of 40–150 cells measured per mouse from several cerebellar slices per mouse. (*E*) Main dendrite width at a distance of one cell-body diameter from the cell body. Statistics are two-way ANOVA. (*F*) Main dendrite length, measured from the middle of the cell body to the first major branch point or, in the absence of that, as far as traceable (see also SI Fig. 10*B*).

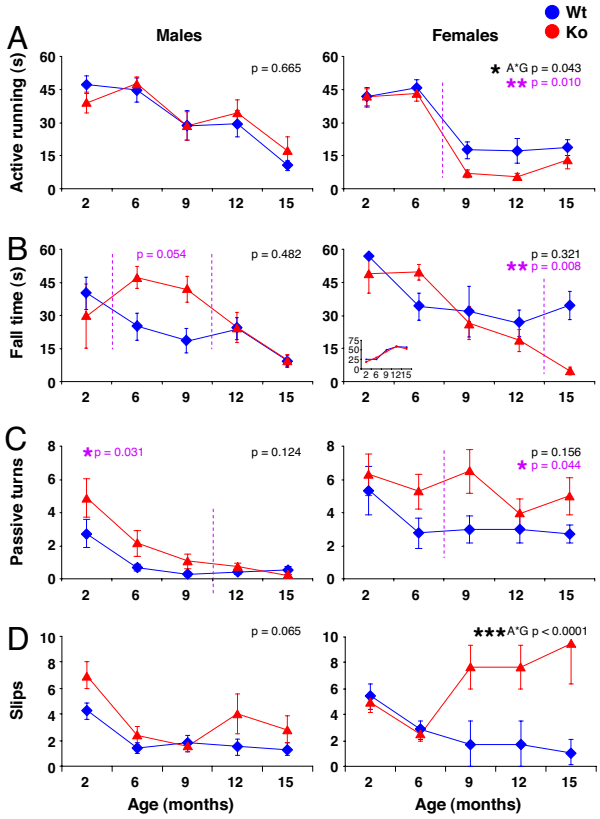

Fig. 3. Rotarod performance is decreased in P-Rex2$^{-/-}$ mice. A cohort of 53 P-Rex2$^{+/+}$ (Wt; blue) and P-Rex2$^{-/-}$ (Ko; red) mice, at least 12 females and 12 males per group, were trained and tested for their performance on the rotarod at different ages as detailed in *Materials and Methods*. Values are from the second run of the performance test. (*A*) Active running: time successfully run on the rod before either turning passively with it or falling off at 42 rpm. (*B*) Fall time: latency to fall at 42 rpm, plotted for animals that fell. Percentage of animals falling is shown in *Inset*. (*C*) Passive turns: number of passive turns clinging to the rod (mean at three top speeds). (*D*) Slips: number of foot slips per animal. All data are mean ± SE; statistics are ANOVA, as detailed in *Materials and Methods*. *P* values in black denote differences between Wt and Ko animals; in purple, those before or after a certain age as indicated by stippled purple lines; and A*G values are those that are significant between genotypes as a function of age.

similar for P-Rex2$^{-/-}$ and P-Rex2$^{+/+}$ mice (data not shown), P-Rex2$^{-/-}$ mice were unable to perform efficiently on the rotarod (Fig. 3 and SI Movie 1). With increasing age, the ability to actively run on the rod (i.e., not to fall off or turn passively clinging on) decreased in P-Rex2$^{-/-}$ females more than in P-Rex2$^{+/+}$ females (Fig. 3*A*), and they also did more passive turning and fell off earlier (Fig. 3 *B* and *C*). The defect in P-Rex2$^{-/-}$ males was more subtle. Although male P-Rex2$^{-/-}$ and P-Rex2$^{+/+}$ mice achieved similar times of active running, P-Rex2$^{-/-}$ males tended to cling on and turn passively with the rod when starting to struggle, rather than falling off (Fig. 3 *B* and *C*). Both male and female P-Rex2$^{-/-}$ mice made significantly more foot slips on the rod than controls (Fig. 3*D*). Again, this defect was greater in females, obvious after the age of 6 months, and bigger in old age. We confirmed the motor coordination defect in the rotarod test in independent experiments with two additional cohorts of mice, one at 2–3 months and one at 9 months of age, which gave similar results (data not shown).

To analyze P-Rex2$^{-/-}$ mouse motor behavior further, we measured basic sensory motor functions in the SHIRPA test (visual placing, negative geotaxis, grip strength, and wire maneuver), which were normal throughout (data not shown). Basic locomotor activity, measured by using infrared-beam-equipped "activity boxes" to record short-range movements of the mice (beam breaks) and runs through the whole box (30), was significantly reduced in P-Rex2$^{-/-}$ mice (SI Fig. 11*A*). For P-Rex2$^{-/-}$ males, this defect became larger with age, whereas in females it was mild but persisted throughout life. To detect gait abnormalities, we analyzed mouse footprint patterns (29, 31). Gait was normal (front-leg gait width, hind-leg gait width, front/hind leg overlap; data not shown), except for stride length that was somewhat reduced in old P-Rex2$^{-/-}$ mice (SI Fig. 11*B*). From 12 months of age, P-Rex2$^{-/-}$ animals had a tendency

PHYSIOLOGY

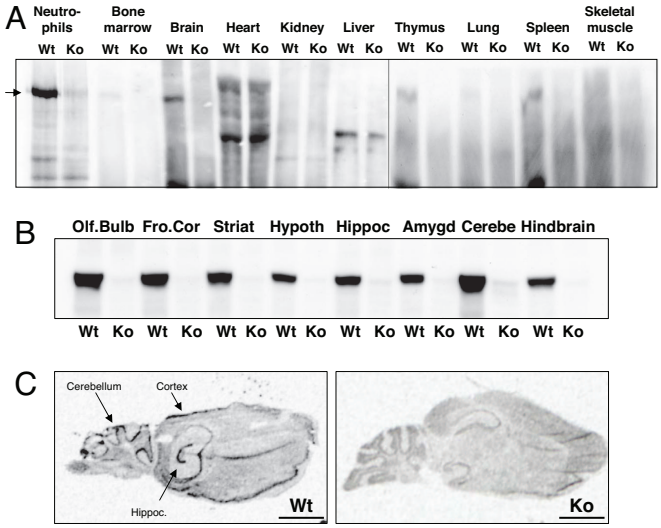

Fig. 4. P-Rex1 is widely distributed within the brain. (*A*) P-Rex1 Western blot with 6F12 mAb of P-Rex1 expression in adult mouse organs and purified BM-derived neutrophils from P-Rex1$^{+/+}$ (Wt) and P-Rex1$^{-/-}$ (Ko) mice. Equal amounts of total lysate protein were loaded. (*B*) Western blot of P-Rex1 distribution in brain sections from adult Wt mice and deletion in P-Rex1$^{-/-}$ (Ko) mice; 500 μg of tissue loaded per lane. (*C*) *In situ* hybridization of adult P-Rex1$^{-/-}$ (Ko) and P-Rex1$^{+/+}$ (Wt) mouse brain slices by using a probe against exon 5 of mouse P-Rex1. (Scale bars, 2 mm.)

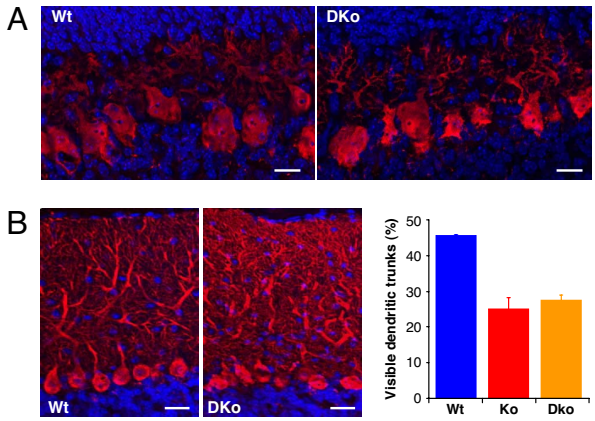

Fig. 5. P-Rex1$^{-/-}$/P-Rex2$^{-/-}$ mice have a defect in Purkinje cell dendrite morphology like P-Rex2$^{-/-}$ mice. (*A*) Morphology of Purkinje cells from P-Rex1$^{-/-}$/P-Rex2$^{-/-}$ pups. Cerebellar slices from 8-day-old P-Rex1$^{-/-}$/P-Rex2$^{-/-}$ (DKo) and Wt mice, fixed, permeabilized, and stained for Calbindin (red) and with Hoechst (blue). Photos are representative of three slices per genotype. (Scale bars, 20 μm.) (*B*) Morphology of Purkinje cells from cerebellar slices of 3-month-old P-Rex1$^{-/-}$/P-Rex2$^{-/-}$ (DKo) and Wt mice. Photos are representative of three slices per genotype. (Scale bars, 10 μm.) Quantification: Cerebellar slices from 3-month-old P-Rex1$^{-/-}$/P-Rex2$^{-/-}$ (DKo, orange), P-Rex2$^{-/-}$ (Ko, red), and P-Rex1$^{+/+}$/P-Rex2$^{+/+}$ mice (Wt; blue) were scored for percentage of Purkinje cells with clearly visible main dendritic trunk as in Fig. 2*D*. At least three cerebellar slices with ≈500 Purkinje cells each were scored per genotype. Data are mean ± range of blind scores from two people.

for limb clasping, holding their hind legs in an abnormally tucked-in position when lifted up by the tail, instead of showing normal escape posture (data not shown). We also tested acoustic startle and prepulse inhibition in our P-Rex2$^{-/-}$ mice, because several proteins involved in these responses have been implicated in cerebellar dysfunction (29, 32–34). We found increased acoustic startle in P-Rex2$^{-/-}$ males throughout life, and this increase was not because of oversensitive or impaired hearing judging by the normal prepulse inhibition (SI Fig. 12*A*). In P-Rex2$^{-/-}$ females, startle was elevated at early age (SI Fig. 12*A*), but this was not confirmed in our second cohort of mice, so may not reflect a true defect (data not shown). To test for potential effects on anxiety levels, we performed elevated plus-maze tests, where animals are given the choice to hide or explore open spaces (35). This showed no defect in P-Rex2$^{-/-}$ mice (SI Fig. 12*B*). We tested for P-Rex2 expression in female versus male cerebellum by Western blotting, which showed no sex-differential P-Rex2 expression (data not shown). To control for potential differences in the estrus cycle of P-Rex2$^{-/-}$ and P-Rex2$^{+/+}$ females, we regularly performed vaginal smear tests that showed no detectable differences (data not shown).

In summary, the P-Rex2$^{-/-}$ mouse has a mild motor coordination defect consistent with cerebellar dysfunction that worsens with age and is more pronounced in females than in males.

P-Rex1 Is Expressed Widely Throughout the Brain, Including the Cerebellum. P-Rex2 is not the only family member in the brain. P-Rex1 expression in the brain, although not as high as in neutrophils, is substantial (Fig. 4*A*). Yoshizawa *et al.* (23) reported the distribution of P-Rex1 within the brain to be widespread. We confirm their findings through P-Rex1 Western blotting of mouse brain slices by using 6F12 mAb (22) (Fig. 4*B*), and P-Rex1 *in situ* hybridization by using a probe against exon 5 (Fig. 4*C*). The expression of P-Rex1 mRNA and protein in the brain is abolished in our P-Rex1$^{-/-}$ mouse (22) (Fig. 4 *B* and *C*). Analysis of Purkinje cell structure by Calbindin staining of cerebellar slices from adult P-Rex1$^{-/-}$ mice (as shown for P-Rex2$^{-/-}$ mice in Fig. 2 *C* and *D*) revealed no defect in the structure of the main dendrite (SI Fig. 13*A*). Similarly, motor behavior tests (rotarod, basic locomotor activity, SHIRPA, and posture tests), which were performed with a cohort of 20 two-month-old P-Rex1$^{-/-}$ and P-Rex1$^{+/+}$ mice (at least four males and four females per genotype) showed no significant motor impairment, although there seemed to be slight tendencies for the P-Rex1$^{-/-}$ mice to perform worse than controls in some tests (SI Fig. 13 *B–D*). Hence, although P-Rex1 is expressed in the cerebellum, P-Rex1 deficiency alone does not cause significant impairments of Purkinje cell structure or motor behavior.

P-Rex1$^{-/-}$/P-Rex2$^{-/-}$ Mice Have a Defect in Purkinje Cell Dendrite Morphology. Western blotting of total brain lysates showed that the levels of P-Rex1 protein are not up-regulated globally in P-Rex2$^{-/-}$ mouse brain, and vice versa (SI Fig. 14*A*). To study possible functional redundancies of P-Rex1 and P-Rex2 in the brain, we generated P-Rex1$^{-/-}$/P-Rex2$^{-/-}$ mice (SI Fig. 14*B*). They were obtained with the expected Mendelian frequency and were viable, fertile, and apparently healthy, although females had significantly higher and males lower body weight than controls (SI Fig. 14*C*). Gross P-Rex1$^{-/-}$/P-Rex2$^{-/-}$ mouse brain anatomy was normal (data not shown). To analyze Purkinje cell morphology in P-Rex1$^{-/-}$/P-Rex2$^{-/-}$ mice, we Calbindin-stained cerebellar slices from 8-day-old and adult animals (Fig. 5). As in P-Rex2$^{-/-}$ mice, Purkinje cell alignment and axon and dendrite outgrowth appeared largely normal in the pups (Fig. 5*A*), but Purkinje cells of adult P-Rex1$^{-/-}$/P-Rex2$^{-/-}$ mice showed the familiar disordered structure of the main dendritic trunk and a disordered appearance of the whole dendritic tree (Fig. 5*B*).

P-Rex1$^{-/-}$/P-Rex2$^{-/-}$ Mice Have a Strong Motor Defect Even at a Young Age. To determine whether P-Rex1 contributes to the control of motor coordination by P-Rex2, we tested a cohort of 43 P-Rex1$^{-/-}$/P-Rex2$^{-/-}$ and control mice (at least 10 males and 8 females per genotype). As with P-Rex2$^{-/-}$ animals of the same age, learning to run on the rotarod was normal in P-Rex1$^{-/-}$/P-Rex2$^{-/-}$ mice (data not shown), and they managed to run actively on the rod for the same time as controls, but both male and female P-Rex1$^{-/-}$/P-Rex2$^{-/-}$ mice did more passive turning and foot slips than

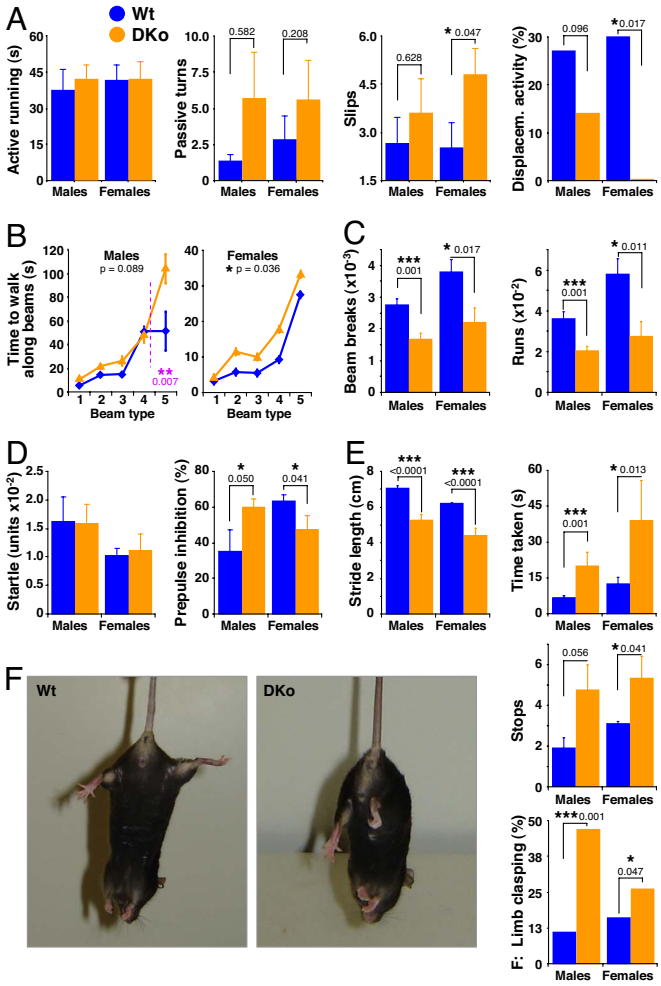

Fig. 6. Motor functions of P-Rex1$^{-/-}$/P-Rex2$^{-/-}$ mice are impaired. A cohort of 43 P-Rex1$^{+/+}$/P-Rex2$^{+/+}$ (Wt; blue) and P-Rex1$^{-/-}$/P-Rex2$^{-/-}$ mice (DKo; orange) (at least 8 females and 10 males per group) were tested at 2–3 months of age for their motor functions. (*A*) Rotarod performance. Active running: time spent running actively at 42 rpm within 60-s trial. Passive turns: number of turns clinging passively to the rod at three top speeds (26, 35, and 42 rpm). Slips: number of foot slips per animal. Displacement activity: standing up, looking up, reversing direction, or grooming at the three lowest speeds (5, 10, and 15 rpm). (*B*) Beam walking. Average time taken to complete the course for increasingly difficult beam types in two trials. (*C*) Basic locomotor activity. Beam breaks and runs in activity boxes, recorded as detailed in *Materials and Methods*. (*D*) Acoustic startle. Mice were exposed to 120-db bursts of white noise with or without 2- to 16-db prepulses and startle was recorded by motion sensors. Startle and inhibition of startle by 16-db prepulses are plotted. (*E*) Footprint analysis. Mouse footprints were analyzed for stride length, time taken to complete the course, and number of stops along the way. (*F*) Limb clasping. P-Rex1$^{-/-}$/P-Rex2$^{-/-}$ mice tended to clasp hind legs instead of showing normal escape posture when lifted by the tail. Data are percentage of animals showing signs of limb clasping as mean ± range of two tests on separate days.

controls (Fig. 6*A*). Furthermore, P-Rex1$^{-/-}$/P-Rex2$^{-/-}$ mice, especially the females, showed fewer displacement activities (standing up, stretching to look up, reversing direction, or grooming), presumably because they had to concentrate harder on staying on the rod (Fig. 6*A*). We had also observed this in P-Rex2$^{-/-}$ females, but the defect was smaller and not always significant (data not shown).

In beam-walking tests, P-Rex1$^{-/-}$/P-Rex2$^{-/-}$ animals took significantly longer than controls to complete the course, females even on wide, "easy" beam types (Fig. 6*B*). Again, we had observed a similar defect in old P-Rex2$^{-/-}$ females but this was only significant for narrow beams (data not shown). Rotarod and beam-walking tests together reveal a motor coordination defect in P-Rex1$^{-/-}$/P-Rex2$^{-/-}$ mice that is stronger than in P-Rex2$^{-/-}$ mice and already apparent at an early age.

Basic locomotor activity was also significantly reduced in P-Rex1$^{-/-}$/P-Rex2$^{-/-}$ mice (Fig. 6*C*), and again, this defect was stronger and apparent earlier than in P-Rex2$^{-/-}$ mice. The basic sensorimotor functions of P-Rex1$^{-/-}$/P-Rex2$^{-/-}$ mice (SHIRPA test) were normal (data not shown), as was their acoustic startle (Fig. 6*D*). Prepulse inhibition seemed altered (Fig. 6*D*), but given the variation observed in this test with P-Rex2$^{-/-}$ mice between different ages and cohorts, we doubt this reflects a true defect. Stride length in P-Rex1$^{-/-}$/P-Rex2$^{-/-}$ mice was significantly reduced, more so at this early age than in 15-month-old P-Rex2$^{-/-}$ animals (Fig. 6*E*). Additionally, P-Rex1$^{-/-}$/P-Rex2$^{-/-}$ animals took longer to walk the footprint course and made more stops along the way than controls (Fig. 6*E*), and also did limb clasping when picked up by the tail (Fig. 6*F*). Again, these were behaviors we only started to notice in very old P-Rex2$^{-/-}$ mice.

In summary, the P-Rex1$^{-/-}$/P-Rex2$^{-/-}$ mice are ataxic and display defects in posture, gait, motor activity, and motor coordination consistent with cerebellar dysfunction that are stronger than in P-Rex1$^{-/-}$ or P-Rex2$^{-/-}$ animals, and apparent even at a young age.

Discussion

Cerebellar dysfunction results in ataxia, a lack of balance and coordination of voluntary movements often with disturbances of posture and gait (28). We have shown here that P-Rex1 and P-Rex2, direct activators of Rac, are expressed in the cerebellum and that they are important regulators of cerebellar morphology and function.

A striking feature of the motor coordination defect in P-Rex2$^{-/-}$ and P-Rex1$^{-/-}$/P-Rex2$^{-/-}$ mice is the sex difference (females worse than males). The sexual dimorphism is most obvious in the rotarod assay, probably because of this being the most taxing task in our battery of tests, revealing defects that are not otherwise obvious. It seems unlikely that female P-Rex-deficient mice simply have lower fitness levels than controls, because P-Rex1$^{-/-}$/P-Rex2$^{-/-}$ mice also showed sexually dimorphic displacement behaviors at slow rotarod settings. Instead, P-Rex may be able respond to sexually dimorphic inputs. The mechanisms governing sex differences in cerebellar development leading to dimorphic motor behavior are unknown (36). In general, sex differences arise from the complex combined effects of gonadal hormone signaling, sex-chromosome-specific gene expression, sexually dimorphic autosomal gene expression, and imprinting (37). P-Rex genes lie on autosomes, and we have no indication that P-Rex is imprinted or sex-differentially expressed in the brain, so it seems likely that gonadal hormones somehow have an impact on P-Rex signaling.

Our aging study enabled us to show that the motor coordination defect in P-Rex2$^{-/-}$ mice worsens with age. A typical feature of inherited ataxias is their progressive worsening, usually attributed to underlying neuronal degeneration, both in humans and in mice (28, 38). Purkinje neurons integrate the electrophysiological input from all other types of cerebellar neurons and generate the total electrophysiological output (26, 27). We found the thinning of the main dendrite in EGFP-P-Rex2$^{-/-}$ Purkinje cells of pups and the disordered appearance of the dendritic trunk in Purkinje cells of adult P-Rex2$^{-/-}$ and P-Rex1$^{-/-}$/P-Rex2$^{-/-}$ mice. This morphology defect most likely arises through perturbation of the underlying actomyosin cytoskeletal structure.

To date, loss- or gain-of-function mutations in 23 seemingly unrelated genes have been identified to cause inherited ataxia in humans or mice (39). Although the pathways leading to cerebellar ataxia are generally still not well understood, it is emerging that many of the proteins encoded by ataxia-causing genes interact with regulators of cell survival and the cytoskeleton (39). It is likely that

PHYSIOLOGY

lack of P-Rex causes ataxia through reduced Rac activity, and the most obvious route is through a defect in the control of Purkinje cell cytoskeletal structure by the Rac/Pak/Wave pathway. Another possibility might be oxidative stress, which has been linked to the pathogenesis of autosomal–recessive human hereditary ataxias such as the common Friedreich ataxia (28). ROS formation requires active Rac, and P-Rex1 regulates ROS formation in neutrophils (21, 22), but ataxia is associated with increased ROS formation and P-Rex deficiency is more likely associated with a decrease. Further work to address the mechanisms underlying the ataxia in P-Rex-deficient mice is underway.

The receptors that couple Purkinje cell stimulation to Rac through P-Rex are unknown. It seems likely that the P-Rex family signals on transactivation of GPCRs with protein-tyrosine kinase-dependent, PI3K-linked, membrane receptors in the brain (18). There are many candidate tyrosine kinase-linked receptors, like the NGF receptor that signals to P-Rex1 in PC12 cells (23). Candidate P-Rex-linked GPCRs in the cerebellum could be glutamate (metabotropic), SDF-1, or sphingosine 1-phosphate receptors (24). In general, GEFs linking GPCRs to Rac activation in the brain are unknown, in contrast to the RGS domain containing GPCR-dependent RhoA-GEFs, which are extensively documented (2). One other GEF has been tested in behavioral assays to date: Ras-GRF1$^{-/-}$ mice have hippocampus-dependent learning and memory defects (40). Ras-GRF1 has dual Ras- and Rac-GEF domains, and it is unknown which confers the behavioral defects (40).

In this article, we have described a function for P-Rex2. With this, we provide a level of knowledge on the pathways regulating cerebellar morphology and function and their deregulation in ataxia. We are now faced with the exciting task of searching for the Purkinje cell receptors that link P-Rex to Rac activation.

Materials and Methods

This section is a summary of the most important techniques used. A detailed description of all methods can be found in *SI Materials and Methods*.

Generation of P-Rex2$^{-/-}$, EGFP-P-Rex2, and P-Rex1$^{-/-}$/P-Rex2$^{-/-}$ Mice. The P-Rex2 gene was targeted by gene-trapping and P-Rex2$^{-/-}$ mice were derived conventionally. EGFP-P-Rex2 mice were generated by crossing EGFP-Pcp2 transgenic mice (The Jackson Laboratory) with P-Rex2$^{-/-}$ mice. P-Rex1$^{-/-}$/P-Rex2$^{-/-}$ mice were generated from P-Rex1$^{-/-}$ and P-Rex2$^{-/-}$ mice.

P-Rex1 and P-Rex2 Western Blots. P-Rex1 Western blots were done with mAb 6F12. For P-Rex2, sheep polyclonal antibodies against amino acids 794–805 and rabbit polyclonal antibodies against amino acids 717–799 of mouse P-Rex2 were raised and affinity-purified.

Cytochemistry, Immunocytochemistry, and Imaging. Cerebella were fixed, sections cut, stained for Calbindin where appropriate, and analyzed by confocal microscopy. High-resolution image analysis was done by using Volocity software.

Behavioral Tests. Behavioral tests were carried out with cohorts of P-Rex2$^{-/-}$, P-Rex1$^{-/-}$, and P-Rex1$^{-/-}$/P-Rex2$^{-/-}$ mice and the appropriate control mice. These tests are described in detail in *SI Materials and Methods*: rotarod, basic locomotor activity, SHIRPA, beam walking, footprint analysis, limb clasping, acoustic startle and prepulse inhibition, and elevated plus-maze.

ACKNOWLEDGMENTS. We thank staff from the Babraham Institute Gene-Targeting Facility, the Small Animal Facility, and Babraham Technix; Ross Miller for the mouse brain cDNA library; Jing Xia for help with Calbindin staining; and Houdini Wu with genotyping. This work was supported by Biotechnology and Biological Sciences Research Council Grant 202/C19943. H.W. is the recipient of Medical Research Council Career Development Award G120/825.

1. Etienne-Manneville S, Hall A (2002) Rho GTPases in cell biology. *Nature* 420:629–635.
2. Govek EE, Newey SE, Van Aelst L (2005) The role of the Rho GTPases in neuronal development. *Genes Dev* 19:1–49.
3. Sugihara K, *et al.* (1998) Rac1 is required for the formation of three germ layers during gastrulation. *Oncogene* 17:3427–3433.
4. Chen L, *et al.* (2007) Rac1 controls the formation of midline commissures and the competency of tangential migration in ventral telencephalic neurons. *J Neurosci* 27:3884–3893.
5. Luo L, *et al.* (1996) Differential effects of the Rac GTPase on Purkinje cell axons and dendritic trunks and spines. *Nature* 379:837–840.
6. Corbetta S, *et al.* (2005) Generation and characterization of Rac3 knockout mice. *Mol Cell Biol* 25:5763–5776.
7. Iwasato T, *et al.* (2007) Rac-GAP alpha-chimerin regulates motor-circuit formation as a key mediator of EphrinB3/EphA4 forward signaling. *Cell* 130:742–753.
8. Soderling SH, *et al.* (2003) Loss of WAVE-1 causes sensorimotor retardation and reduced learning and memory in mice. *Proc Natl Acad Sci USA* 100:1723–1728.
9. Rossman KL, Der CJ, Sondek J (2005) GEF means go: Turning on RHO GTPases with guanine nucleotide-exchange factors. *Nat Rev Mol Cell Biol* 6:167–180.
10. Tolias KF, *et al.* (2007) The Rac1 guanine nucleotide exchange factor Tiam1 mediates EphB receptor-dependent dendritic spine development. *Proc Natl Acad Sci USA* 104:7265–7270.
11. Cowan CW, *et al.* (2005) Vav family GEFs link activated Ephs to endocytosis and axon guidance. *Neuron* 46:205–217.
12. Katoh H, Negishi M (2003) RhoG activates Rac1 by direct interaction with the Dock180-binding protein Elmo. *Nature* 424:461–464.
12. Watabe-Uchida M, John KA, Janas JA, Newey SE, Van Aelst L (2006) The Rac activator DOCK7 regulates neuronal polarity through local phosphorylation of stathmin/Op18. *Neuron* 51:727–739.
14. Bryan B, *et al.* (2004) GEFT, a Rho family guanine nucleotide exchange factor, regulates neurite outgrowth and dendritic spine formation. *J Biol Chem* 279:45824–45832.
15. Zhang H, Webb DJ, Asmussen H, Horwitz AF (2003) Synapse formation is regulated by the signaling adaptor GIT1. *J Cell Biol* 161:131–142.
16. Jacquier A, *et al.* (2006) Alsin/Rac1 signaling controls survival and growth of spinal motoneurons. *Ann Neurol* 60:105–117.
17. Kanekura K, *et al.* (2005) A Rac1/phosphatidylinositol 3-kinase/Akt3 anti-apoptotic pathway, triggered by AlsinLF, the product of the ALS2 gene, antagonizes Cu/Zn-superoxide dismutase (SOD1) mutant-induced motoneuronal cell death. *J Biol Chem* 280:4532–4543.
18. Welch HC, *et al.* (2002) P-Rex1, a PtdIns(3,4,5)P3- and Gbetagamma-regulated guanine-nucleotide exchange factor for Rac. *Cell* 108:809–821.
19. Donald S, *et al.* (2004) P-Rex2, a new guanine-nucleotide exchange factor for Rac. *FEBS Lett* 572:172–176.
20. Rosenfeldt H, Vazquez-Prado J, Gutkind JS (2004) P-REX2, a novel PI-3-kinase sensitive Rac exchange factor. *FEBS Lett* 572:167–171.
21. Dong X, *et al.* (2005) P-Rex1 is a primary Rac2 guanine nucleotide exchange factor in mouse neutrophils. *Curr Biol* 15:1874–1879.
22. Welch HC, *et al.* (2005) P-Rex1 regulates neutrophil function. *Curr Biol* 15:1867–1873.
23. Yoshizawa M, *et al.* (2005) Involvement of a Rac activator, P-Rex1, in neurotrophin-derived signaling and neuronal migration. *J Neurosci* 25:4406–4419.
24. Li Z, Paik JH, Wang Z, Hla T, Wu D (2005) Role of guanine nucleotide exchange factor P-Rex-2b in sphingosine 1-phosphate-induced Rac1 activation and cell migration in endothelial cells. *Prostaglandins Other Lipid Mediat* 76:95–104.
25. Tomomura M, Rice DS, Morgan JI, Yuzaki M (2001) Purification of Purkinje cells by fluorescence-activated cell sorting from transgenic mice that express green fluorescent protein. *Eur J Neurosci* 14:57–63.
26. Hesslow G, Yeo C (1998) Cerebellum and learning: a complex problem. *Science* 280:1817–1819.
27. Thach WT (1998) A role for the cerebellum in learning movement coordination. *Neurobiol Learn Mem* 70:177–188.
28. Taroni F, DiDonato S (2004) Pathways to motor incoordination: the inherited ataxias. *Nat Rev Neurosci* 5:641–655.
29. Carter RJ, *et al.* (1999) Characterization of progressive motor deficits in mice transgenic for the human Huntington's disease mutation. *J Neurosci* 19:3248–3257.
30. Colebrooke RE, *et al.* (2006) Age-related decline in striatal dopamine content and motor performance occurs in the absence of nigral cell loss in a genetic mouse model of Parkinson's disease. *Eur J Neurosci* 24:2622–2630.
31. Brunskill EW, *et al.* (2005) Abnormal neurodevelopment, neurosignaling and behaviour in Npas3-deficient mice. *Eur J Neurosci* 22:1265–1276.
32. Swerdlow NR, Geyer MA, Braff DL (2001) Neural circuit regulation of prepulse inhibition of startle in the rat: current knowledge and future challenges. *Psychopharmacology (Berl)* 156:194–215.
33. Beglopoulos V, *et al.* (2005) Neurexophilin 3 is highly localized in cortical and cerebellar regions and is functionally important for sensorimotor gating and motor coordination. *Mol Cell Biol* 25:7278–7288.
34. Takeuchi T, *et al.* (2001) Roles of the glutamate receptor epsilon2 and delta2 subunits in the potentiation and prepulse inhibition of the acoustic startle reflex. *Eur J Neurosci* 14:153–160.
35. Plagge A, *et al.* (2005) Imprinted Nesp55 influences behavioral reactivity to novel environments. *Mol Cell Biol* 25:3019–3026.
36. Nguon K, Ladd B, Baxter MG, Sajdel-Sulkowska EM (2005) Sexual dimorphism in cerebellar structure, function, and response to environmental perturbations. *Prog Brain Res* 148:341–351.
37. Davies W, Wilkinson LS (2006) It is not all hormones: Alternative explanations for sexual differentiation of the brain. *Brain Res* 1126:36–45.
38. Grusser-Cornehls U, Baurle J (2001) Mutant mice as a model for cerebellar ataxia. *Prog Neurobiol* 63:489–540.
39. Lim HT, *et al.* (2006) A protein-protein interaction network for human inherited ataxias and disorders of Purkinje cell degeneration. *Cell* 125:801–814.
40. Giese KP, *et al.* (2001) Hippocampus-dependent learning and memory is impaired in mice lacking the Ras-guanine-nucleotide releasing factor 1 (Ras-GRF1) *Neuropharmacology* 41:791–800.